Regular Article

PLATELETS AND THROMBOPOIESIS

CEACAM2 negatively regulates hemi (ITAM-bearing) GPVI and CLEC-2 pathways and thrombus growth in vitro and in vivo

Musaed M. Alshahrani,[1] Eunice Yang,[1] Jana Yip,[1] Simona S. Ghanem,[2] Simon L. Abdallah,[2] Anthony M. deAngelis,[2] Cindy J. O'Malley,[1] Fatemeh Moheimani,[1] Sonia M. Najjar,[2] and Denise E. Jackson[1]

[1]Thrombosis and Vascular Diseases Laboratory, Health Innovations Research Institute, School of Medical Sciences, Royal Melbourne Institute of Technology University, Bundoora, VIC, Australia; and [2]Center for Diabetes and Endocrine Research, Department of Physiology and Pharmacology, College of Medicine and Life Sciences, University of Toledo, Toledo, OH

Key Points

- CEACAM2 is a novel platelet immunoreceptor.
- CEACAM2 negatively regulates platelet-collagen interactions and thrombus growth and stability in vitro, in vivo and CLEC-2 pathways.

Carcinoembryonic antigen–related cell adhesion molecule-2 (CEACAM2) is a cell-surface glycoprotein expressed on blood, epithelial, and vascular cells. CEACAM2 possesses adhesive and signaling properties mediated by immunoreceptor tyrosine-based inhibitory motifs. In this study, we demonstrate that CEACAM2 is expressed on the surface and in intracellular pools of platelets. Functional studies of platelets from $Ceacam2^{-/-}$-deficient mice ($Cc2^{-/-}$) revealed that CEACAM2 serves to negatively regulate collagen glycoprotein VI (platelet) (GPVI)-FcRγ–chain and the C-type lectinlike receptor 2 (CLEC-2) signaling. $Cc2^{-/-}$ platelets displayed enhanced GPVI and CLEC-2–selective ligands, collagen-related peptide (CRP), collagen, and rhodocytin (Rhod)-mediated platelet aggregation. They also exhibited increased adhesion on type I collagen, and hyperre-sponsive CRP and CLEC-2–induced α and dense granule release compared with wild-type platelets. Furthermore, using intravital microscopy to ferric chloride (FeCl$_3$)–injured mesenteric arterioles and laser-induced injury of cremaster muscle arterioles, we herein show that thrombi formed in $Cc2^{-/-}$ mice were larger and more stable than wild-type controls in vivo. Thus, CEACAM2 is a novel platelet immunoreceptor that acts as a negative regulator of platelet GPVI-collagen interactions and of ITAM receptor CLEC-2 pathways. (Blood. 2014;124(15):2431-2441)

Introduction

Many negative regulatory mechanisms down-modulate in vivo platelet-collagen interactions. Major regulators include nitric oxide and prostacyclin,[1] expressed by the endothelium, and members of the immunoglobulin (Ig) immunoreceptor tyrosine–based inhibitory motif (ITIM) superfamily, contained within platelets. The latter group includes platelet endothelial cell adhesion molecule–1 (PECAM-1) and carcinoembryonic antigen–related cell adhesion molecule–1 (CEACAM1), which autoregulate platelet interactions in the presence of collagen.[2-5] Collagen plays a role in platelet adhesion and thrombus development, especially with glycoprotein-VI (GPVI)/ Fc receptor (FcR)γ-chain signaling. Thus, natural inhibitors of the autoregulatory mechanisms moderating signaling processes between the GPVI/FcRγ-chain and collagen must be present in platelets.

The ITIM-bearing receptor regulation of immunoreceptor tyrosine-based activation motif (ITAM) in leukocytes is well understood. However, less is known about regulation in platelets where Ig-ITIM–bearing receptors bind with multiple phosphatase types, including SH2-containing protein-tyrosine phosphatase-1 and -2 (SHP-1, SHP-2) and SH2 domain–containing inositol polyphos-phate 5′-phosphatase (SHIP).[6] Current theories suggest that Ig-ITIM–bearing receptors undergo differential interaction with distinct phosphatase groups in a manner depending on cell conditions and activation status.[7,8]

Regulation of these complex inhibitory mechanisms is difficult to dissect out, because under certain conditions, inhibitory ITAM signaling is mediated by ITAM-bearing receptors via the FcRγ-chain or DAP12 adaptor.[9,10] Switching between ITAM signaling activa-tion and inhibition is governed by the strength of ligand binding to the receptor. Low-avidity ligand interactions may influence regulation of inhibitory signaling by phosphatases. Conversely, higher-avidity ligand cross-linkages may activate ITAM-mediated signaling responses. Hence, understanding the complex relationship between activation and inhibition in platelets is crucial.[9,10]

In murine platelets, there are 2 hemi ITAM–associated signaling pathways, collagen GPVI-FcRγ–chain and the C-type lectin-like receptor 2 (CLEC-2). The snake venom protein rhodocytin is a CLEC-2 ligand that induces CLEC-2 clustering and platelet activation. The CLEC-2 receptor induces activation-dependent signaling through a similar GPVI-FcRγ–chain pathway. However, CLEC-2 signals rely more on Syk rather than Src tyrosine kinases and the PLCγ2-dependent mechanism of platelet activation.[11,12]

Several studies imply that Ig-ITIM superfamily members in platelets regulate platelet-collagen interactions. Human and murine platelets do not contain the prototypic inhibitory Ig-ITIM superfam-ily member FcγRIIb, but instead, PECAM-1 and CEACAM1 Ig-ITIM-superfamily members capable of negatively regulating platelet

---

There is an Inside Blood Commentary on this article in this issue.

interactions with collagen.[2,3,13] Other Ig-ITIM superfamily members, including triggering receptors expressed on myeloid cells (TREM), transcript-1 (TLT-1), and G6B, are critical for modulating platelet function.[14,15] Much remains to be investigated to assess the contribution of Ig-ITIM superfamily in platelet thrombus formation.

CEACAM2 (previously known as Bgp2) is a type I transmembrane receptor from the CEACAM superfamily of genes that is expressed in few cell types, including intestinal tissue crypt epithelia, kidney cells, testis, and several nuclei in the brain, including the ventromedial hypothalamus.[16-18] CEACAM1 and CEACAM2 proteins, encoded by different genes containing 9 exons each,[19] share a similar overall structure in particular with respect to Ig-Domains in the extracellular segment and an almost identical ITIM-containing cytoplasmic tail. However, the 2 proteins differ by 2 important features. First, CEACAM1 predominantly possesses 4 extracellular Ig-Domains (CEACAM1-4L), in contrast to CEACAM2, which has 2 extracellular Ig domains (N terminal, A2 domain), resulting from alternative splicing of exons 3 and 4 (CEACAM2-2L).[18] This leads to a differential degree of glycosylation with CEACAM2 containing 5 of the 16 N-linked glycans in CEACAM1. Second, the 2 receptors display differential ligand-binding properties of the distal variable N-terminal Ig domain that promotes homophilic binding in CEACAM1, but not CEACAM2.[20] The only ligand thus far identified for CEACAM2 is the murine coronavirus mouse hepatitis virus spike glycoprotein(s). In addition, CEACAM proteins use 2 ITIMs to recruit SHP-1 and, to a lesser degree, SHP-2 protein-tyrosine phosphatase.[21,22] With SHP-1 playing an important role in platelet activation by the collagen receptor glycoprotein VI,[23] it is likely that SHP recruitment to the ITIM domains of CEACAM1 contributes to the regulatory role of CEACAM1 in platelet-collagen interaction.[13]

Potential involvement of CEACAM2 in regulating platelet-collagen interactions, CLEC-2 signaling, and thrombus formation is poorly understood. Thus, the current studies investigated whether CEACAM2 regulates platelet-collagen interactions, both in vitro and in vivo, as well as CLEC-2–dependent pathways.

Materials and methods

Antibodies and chemicals

The specific rabbit anti-mouse CEACAM2 polyclonal antibody (2052)[16] and CEACAM1 antibody (2457)[13,24] were previously described. PECAM-1 antibody (anti-mouse, 390) was provided by Dr Steve Albelda (Philadelphia, PA).[25] Anti-rabbit fluorescein isothiocyanate (FITC) and rabbit anti-mouse phycoerythrin (PE) were purchased from Dako (Botany, Australia). Anti-mouse GPVI,[26] anti-mouse integrin $\alpha_2\beta_1$ (CD49b),[27] anti-mouse GPIbα-IX-V complex (CD42b),[28] and anti-mouse GPVI (JAQ1)[29] were purchased from Emfret Analytics (Würzburg, Germany). Anti-mouse integrin $\alpha_{IIb}\beta_3$ (CD61),[30] anti-mouse CD44,[31] isotype control antibody CD3$_\epsilon$, and horseradish peroxidase (HRP)–conjugated anti-phosphotyrosine-RC20 antibodies were obtained from BD Biosciences Pharmingen (Franklin Lakes, NJ). Anti-phosphotyrosine 4G10 antibody was obtained from Millipore (Billerica, MA). Rabbit anti-Akt-(#9272), anti-phospho-Akt-(S473, #4060), anti-phospho-Src-(Tyr416), and anti-Src-(36D10) antibodies were purchased from Cell Signaling Technology (Danvers, MA). Anti-mouse CD9,[32] PLCγ2 (sc-407), Syk (c-20; sc-929), ERK-2, and GAPDH-(sc-32233) antibodies were purchased from Santa Cruz Biotechnology (Dallas, TX). Rhodocytin snake venom protein was kindly donated by Professor Bernard Nieswandt (Rudolf Virchow Center, Würzburg, Germany).

Mice

The generation of $Cc2^{-/-}$ mice and breeding onto C57BL/6 background for 10 generations has been described.[16] Wild-type C57BL/6 mice were purchased from Animal Resources Centre animal facility (Perth, WA). Age- and sex-matched wild-type and $Cc2^{-/-}$ littermates were housed at the Royal Melbourne Institute of Technology (RMIT) University animal facility. All procedures were approved by the RMIT University Animal Ethics Committee #0918 and #1239.

Hematologic parameters

Hematologic parameters were determined on ethylenediamine tetraacetic acid samples collected from wild-type and $Cc2^{-/-}$ mice using an Emerald hematology analyzer (Abbott, IL). One-hundred white blood cell (WBC) differentials were performed and expressed as percentage and absolute count ($\times 10^9$/L).

Platelet preparation

Platelet-rich plasma (PRP) and washed murine platelets were isolated as previously described.[33]

Platelet aggregation

Platelet aggregation responses were measured on a 4-channel light transmission aggregometer as previously described.[34,35]

Flow cytometry

Surface and total expression of CEACAM2 in wild-type and $Cc2^{-/-}$ platelets were performed using washed platelets; for total expression, platelets were resuspended in 0.1% (weight/volume [wt/vol]) saponin as previously described[13,36] and rabbit anti-mouse CEACAM2 antibody 2052 (1/100).

Dense granule release using quinacrine uptake

Dense granule release was performed as previously described.[2] Dense granule exocytosis was recorded as the percentage decrease in quinacrine fluorescence intensity compared with resting platelets. 10 000 individual platelets were analyzed on a FACS Canto II flow cytometer and by Weasel software (version 3.0.2)

Static platelet adhesion on type I collagen

A time course of static platelet adhesion was performed for wild-type and $Cc2^{-/-}$ platelets as previously described.[34]

Immunoprecipitation and immunoblotting

Immunoprecipitation and immunoblotting were performed as previously described.[2,17]

In vivo thrombosis models

Ferric chloride–induced injury of mesenteric arterioles (80-100 μm),[13] laser induced injury of cremaster muscle arterioles (30-40 μm),[37,38] and GPVI depletion using JAQ1 antibody[29] were performed as previously described.

Analysis of murine platelet adhesion and thrombus formation under in vitro arterial flow

A 3-channel μ-slide III$^{0.1}$ with dimensions 0.1 $\times$ 1.0 $\times$ 45 mm (height $\times$ width $\times$ length) (microslides, ibidi, Martinsried, Germany) were coated with 500 μg/mL type I fibrillar collagen (Nycomed) for 1 hour at 37°C. Whole blood from wild-type and $Cc2^{-/-}$ mice was normalized to 3 $\times$ 10^8/mL platelets and then incubated with 0.05% (wt/vol) rhodamine 6G dye for 30 minutes at 37°C. Labeled whole blood was perfused through the collagen-coated μ-slide-III$^{0.1}$ at a shear wall flow rate of 1800 s^{-1} for 4 minutes. Nonadherent cells were removed by the flow of Ringer-citrate-dextrose (RCD) buffer (pH 7.4) at the same shear wall flow rate. Thrombi were recorded in real time using Z-stack analysis, and deconvolution of 3-D reconstructions were recorded using a Zeiss Axiovert microscope and Axiovision Rel4.6 software. Thrombus volume was calculated from the thrombus area (μm^2) multiplied by the thrombus height (μm) for wild-type and $Cc2^{-/-}$ at various time points.

Table 1. Summary of peripheral blood hematologic parameters for wild-type and $Cc2^{-/-}$ mice

Hematologic parameter	Wild-type (n = 6)	$Cc2^{-/-}$ (n = 6)
WBC, $\times 10^9$/L	6.20 ± 1.03	5.25 ± 0.66
RBC, $\times 10^{12}$/L	9.07 ± 0.22	8.89 ± 0.46
HGB, g/L	132.33 ± 3.08	129.33 ± 6.90
PCV, L/L	0.43 ± 0.01	0.42 ± 0.02
MCV, fl	48.33 ± 0.55	48.00 ± 0.85
MCH, pg	14.61 ± 0.24	14.56 ± 0.23
MCHC, $\times 10^3$ g/L	302.00 ± 3.40	303.83 ± 3.21
RDW, %	13.25 ± 0.18	13.58 ± 0.19
PLT, $\times 10^9$/L	726.66 ± 23.10	741.00 ± 9.80
WBC/Neut/, %	8.58 ± 1.72	7.41 ± 1.50
WBC/Lymph, %	88.91 ± 2.34	90.00 ± 2.27
WBC/Mono, %	2.50 ± 0.65	3.08 ± 1.26
WBC/Neut, $\times 10^9$/L	0.55 ± 0.17	0.37 ± 0.07
WBC/Lymph, $\times 10^9$/L	5.47 ± 0.88	4.74 ± 0.65
WBC/Mono, $\times 10^9$/L	0.17 ± 0.06	0.16 ± 0.07

Hematologic parameters were analyzed from wild-type and $Cc2^{-/-}$ whole blood. Hgb, hemoglobin; PCV, packed cell volume; MCV, mean cell volume; MCH, mean cell hemoglobin; MCHC, mean cell hemoglobin concentration; PLT, platelets; Neut, neutrophils; Lymph, lymphocytes; Mono, monocytes. The assays were run in triplicate, and the data shown are representative of 6 independent experiments and presented as MFI ± standard error of the mean (SEM) ($P > .05$ is nonsignificant for all hematologic parameters) using statistics Student t test.

Statistical analysis

Data were checked for normal distribution using the Shapiro-Wilks normality test, and statistical significance was determined using unpaired Student t test and 2-way analysis of variance. P values <.05 were considered significant. Data were analyzed by using GraphPad Prism software program, version 5 (GraphPad, San Diego, CA).

Results

Ceacam2-null mice have normal hematopoiesis parameters

To determine whether *Ceacam2* deletion affects production of hematopoietic cells such as platelets, cells from sex- and age-matched wild-type and $Cc2^{-/-}$ mice were compared. As Table 1 reveals, all hematologic parameters including hemoglobin (Hb) as well as WBC, red blood cell (RBC), and platelet counts were normal in $Cc2^{-/-}$ compared with wild-type mice ($P > .05$; n = 6).

CEACAM2 is expressed on the surface and in the intracellular pool of murine platelets

Next, we investigated the cellular compartmentalization of CEACAM2 in resting murine platelets. To determine whether CEACAM2 is expressed at the surface membrane and whether this is increased after granule release, we examined the binding of a specific anti-mouse CEACAM2 polyclonal antibody to resting and agonist-stimulated wild-type mouse platelets, detected by flow cytometry. As shown in Figure 1A, resting platelets incubated with the anti-mouse CEACAM2 antibody exhibited a twofold increase in surface expression compared with normal rabbit preimmune serum (21.56 ± 1.754 vs 9.854 ± 1.597, respectively; **$P < .01$; n = 5). This finding indicates the presence of CEACAM2 on the surface of mouse platelets. In addition, characterization of the total distribution of CEACAM2 in mouse platelets was determined by permeability of the platelet membrane with saponin. Saponin-treated platelets incubated with anti-CEACAM2 antibody exhibited a 2.5-fold higher mean fluorescence intensity (MFI) than those incubated with normal

rabbit preimmune serum (83.66 ± 8.935 vs 33.08 ± 6.756, respectively; **$P < .01$; n = 5; Figure 1A). This finding points to an additional intracellular CEACAM2 pool in murine platelets. CEACAM2 is predominantly expressed in platelets as the commonly found CEACAM2-2L (CC2-2L) form of ~52 kDa (Figure 1C). CC2-2L of CEACAM2 contains 2 Ig-Domains (N terminal, A2 domain), a transmembrane domain, and long ITIM-containing cytoplasmic domain. Cell-surface expression of CEACAM2 was increased in a dose-responsive manner upon agonist stimulation with thrombin, protease-activated receptor-4 agonist peptide (PAR-4), and collagen-related peptide (CRP) compared with resting platelets (***$P < .001$; n = 4; Figure 1B). Whereas CEACAM2 was absent in $Cc2^{-/-}$ platelets (Figure 1D), the expression of several platelet glycoproteins, including GPVI, PECAM-1, CEACAM1, integrin $\alpha_2\beta_1$, integrin $\alpha_{IIb}\beta_3$, GPIb-IX-V complex, CD44, and CD9, was similar to that in wild-type platelets (Figure 1D-F). Consistently, upregulation of CEACAM1 surface expression was similar in wild-type and $Cc2^{-/-}$ platelets in a dose-dependent manner in response to thrombin, PAR-4 agonist peptide, and CRP (Figure 1G). These data show that CEACAM2 is localized to both the surface and the intracellular pool in resting murine platelets.

Ceacam2-null platelets are hyperresponsive to GPVI and CLEC-2–selective agonists

Next, we examined whether CEACAM2 negatively regulates ITAM-bearing, collagen-GPVI and CLEC-2–mediated platelet response. To this end, wild-type and $Cc2^{-/-}$ platelets were stimulated using a range of G-protein–coupled agonists (PAR-4 agonist peptide; 100-300 μM; Figure 2Aa-c), adenosine diphosphate (ADP; 2.5-10 μM; Figure 2Ad-f), and calcium ionophore (CI-A23187; 1.25-5.0 μg/mL; Figure 2Ag-i), with acid-soluble type I collagen (1.5-4 μg/mL; Figure 2Aj-l), the GPVI collagen receptor selective agonist, CRP (0.62-2.5 μg/mL; Figure 2Am-o), and the CLEC-2 receptor agonist, Rhod (0.12-0.48 μg/mL; Figure 2Ap-r). As is shown in Figure 2A-B, similar platelet aggregation profiles were observed in wild-type and $Cc2^{-/-}$ platelets treated with PAR-4 agonist peptide, ADP and CI. However, in response to collagen, CRP, and Rhod agonist, stimulation of platelet aggregation was observed in $Cc2^{-/-}$ platelets, particularly at subthreshold doses compared with wild-type platelets. These data suggest that lack of CEACAM2 leads to hyperresponsive tyrosine-kinase–dependent signaling pathway in platelets upon collagen, CRP, and Rhod stimulation.

Ceacam2-null platelets demonstrate enhanced α and dense granule secretion

Because $Cc2^{-/-}$ platelets exhibited hyperresponsive GPVI- or CLEC-2–mediated platelet aggregation responses, we investigated whether lack of CEACAM2 affects the platelet-release reaction stimulated by the GPVI-specific agonist, CRP. The ability of wild-type and $Cc2^{-/-}$ platelets to secrete α (P-selectin) and dense granule (Quinacrine) upon GPVI and CLEC-2 stimulation was determined. As is seen in Figure 3A-B, $Cc2^{-/-}$ platelets released more α and dense granules at all doses of CRP and Rhod compared with wild-type platelets, but not when treated with thrombin and PAR-4 agonist peptide at any dose (*$P < .05$, **$P < .01$, ***$P < .001$; n = 4). Interestingly, $Cc2^{-/-}$ platelets released similar α granules upon CRP stimulation compared with $Cc1^{-/-}$ platelets (Figure 3Ab). Moreover, $Cc2^{-/-}$ platelets released similar α and dense granules upon Rhod stimulation compared with $Cc1^{-/-}$ platelets (Figure 3Ac-Bc). These results support the hypothesis that CEACAM2 acts as a negative regulator of GPVI and CLEC-2–mediated platelet granule release.
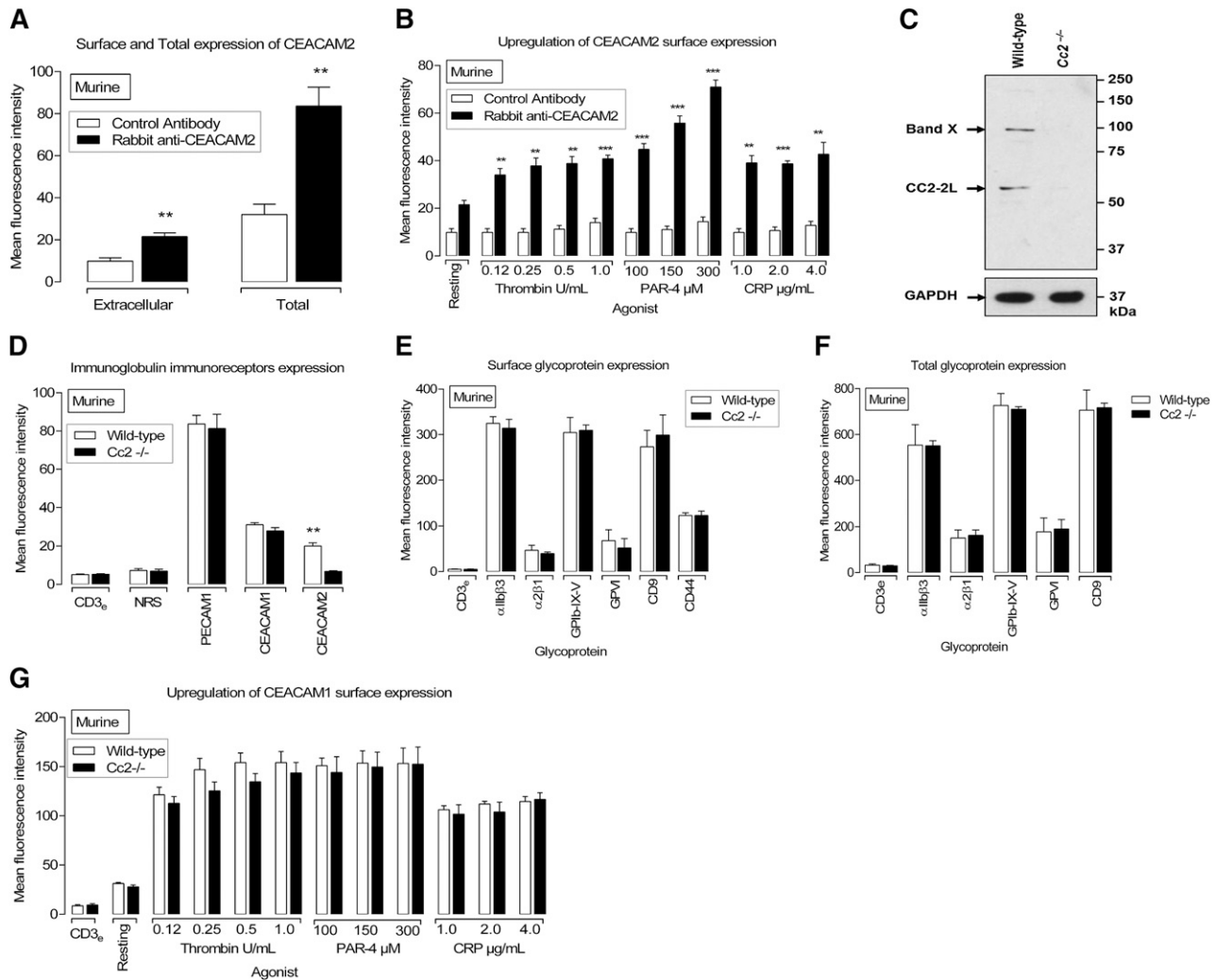
Figure 1. CEACAM2 is expressed on the surface and in intracellular pools in murine platelets. (A) Flow cytometric analysis of CEACAM2 surface and total expression on resting murine platelets. Platelets were stained with a polyclonal anti-murine CEACAM2 2052 antibody followed by a secondary PE-conjugated anti-rabbit antibody. Normal rabbit serum was included as a negative control. For total expression, platelets were resuspended in 0.1% (wt/vol) saponin and then washed with a combination of 0.1% (wt/vol) saponin and 0.2% (wt/vol) bovine serum albumin. Data were collected by a live platelet gate based on forward vs side scatter profiles on a FACS Canto II flow cytometer. Results are cumulative data derived from 4 independent experiments and represented as mean fluorescence intensity (MFI) ± SEM (**$P < .01$; n = 4). (B) CEACAM2 surface expression upon agonist stimulation of murine platelets using thrombin (0.125-1.0 U/mL), PAR-4 agonist peptide (100-300 μM), and collagen-related peptide (CRP; 1.0-4.0 μg/mL) over a dose-dependent range (**$P < .01$ and ***$P < .001$; n = 4). CEACAM2 surface expression was determined as described in (A). (C) Platelet lysates from wild-type and $Cc2^{-/-}$ mice were analyzed by 10% sodium dodecyl sulfate polyacrylamide gel electrophoresis (SDS-PAGE) and western blotting using 1:2000 of rabbit anti-mouse CEACAM2 polyclonal antibody (2052) (upper panel), followed by reprobing with GAPDH antibody to control for protein loading (bottom panel). A ~52-kDa band representing CEACAM2 and another one (band X) at ~95kDa representing an unidentified protein were detected. (D) Flow cytometric analysis of PECAM-1, CEACAM1, and CEACAM2 expression on resting wild-type vs $Cc2^{-/-}$ platelets. Wild-type and $Cc2^{-/-}$ platelets were stained with a monoclonal anti-murine PECAM-1 antibody, polyclonal anti-murine CEACAM1 2457 antibody, or polyclonal anti-murine CEACAM2 2052 antibody followed by a secondary PE-conjugated anti-rat or anti-rabbit antibody. Normal rabbit serum (NRS) and isotype control antibody CD3 were included as negative controls. Data were collected by a live platelet gate based on forward vs side scatter profiles on a FACS Canto II flow cytometer. Results are cumulative data derived from 4 independent experiments and represented as MFI ± SEM (**$P < .01$; n = 4). (E) Cell-surface expression of platelet glycoproteins was monitored by flow cytometry using specific monoclonal antibodies for wild-type and $Cc2^{-/-}$ platelets. Platelets were preincubated with anti-mouse integrin β_3, CD61 (10 μg/mL), anti-mouse integrin $\alpha_2\beta_1$, CD49b (15 μg/mL), anti-mouse GPIbα/IX/V, CD42b (10 μg/mL), anti-mouse CD44 (10 μg/mL), anti-mouse GPVI (10 μg/mL), and anti-mouse CD9 (10 μg/mL). MFI was reported with an SEM for at least 4 independent experiments and no significant difference demonstrated. (F) Total expression of platelet glycoproteins on resting wild-type and $Cc2^{-/-}$ murine platelets was determined as described in (A). Antibodies concentrations were described in (E). (G) Cell-surface expression of CEACAM1 upon agonist stimulation of wild-type vs $Cc2^{-/-}$ murine platelets was determined as described in (B).

Ceacam2-null platelets display increased static adhesion to immobilized type I fibrillar collagen

We examined whether CEACAM2 modulates collagen-GPVI–mediated platelet response in a manner similar to other platelet immunoreceptors. Static platelet adhesion on type I fibrillar collagen was performed to determine the binding characteristics of platelets derived from wild-type and $Cc2^{-/-}$ mice over time. *Ceacam2*-null platelets bound more to immobilized type I fibrillar collagen but not negative control (RCD buffer) compared with wild-type platelets at all time points (*$P < .05$, **$P < .01$, ***$P < .001$; n = 3; Figure 4).

Together, this reveals that upon static adhesion to immobilized type I collagen, $Cc2^{-/-}$ platelets exhibited a hyperresponsive platelet adhesion compared with wild-type platelets.

Tyrosine phosphorylation including PLCγ2, Src and Syk is enhanced in $Cc2^{-/-}$ platelets after CRP stimulation and PLCγ2, Syk after Rhod stimulation

To determine whether CEACAM2 plays a negative regulatory role in ITAM-signaling pathways in platelets, wild-type and $Cc2^{-/-}$ platelets were stimulated using 10 μg/mL of CRP over a 3-minute
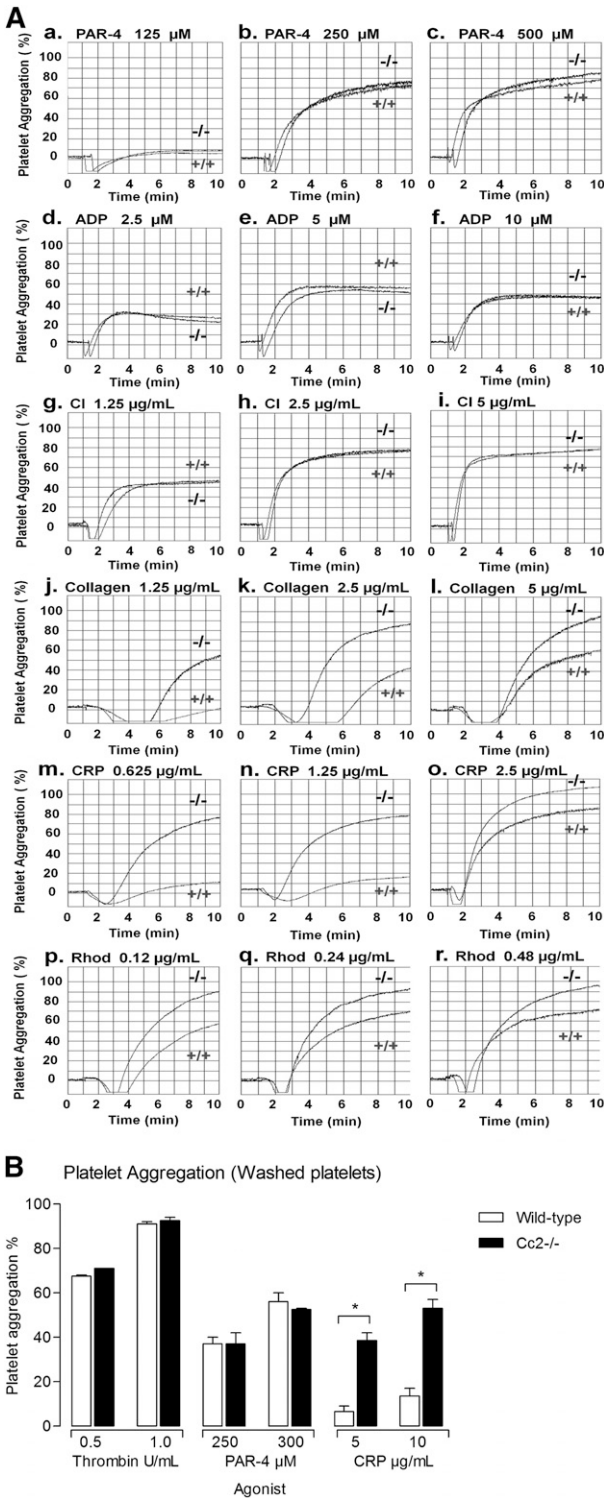
A

B

Figure 2. $Cc2^{-/-}$ **platelets are hyperresponsive to stimulation with type I collagen, GPVI, and CLEC-2–selective agonists, CRP and Rhod.** (A) Aggregation responses of PRP (platelet count adjusted to 1×10^8/mL) for wild-type ($^{+/+}$) and $Cc2^{-/-}$ mice were determined after stimulation with the following agonists: (a-c) PAR-4 agonist peptide (125-500 μM); (d-f) ADP (2.5-10 μM); (g-i) calcium ionophore (1.25-5 μg/mL); (j-l) type I collagen (1.25-5 μg/mL); (m-o) CRP (0.625-2.5 μg/mL); and (p-r) Rhod (0.12-0.48 μg/mL). Note that $Cc2^{-/-}$ platelets are hyperresponsive to stimulation by type I collagen, GPVI, and CLEC-2–selective agonists, CRP and Rhod. These data are representative of at least 4 independent experiments performed. (B) Aggregation responses of washed platelets for wild-type and $Cc2^{-/-}$ mice were determined after stimulation with the following agonists: thrombin (0.25-1 U/mL), PAR-4 agonist peptide (250-500 μM), and CRP (5-10 μg/mL). Note that $Cc2^{-/-}$ platelets are hyperresponsive to stimulation by GPVI-selective agonist, CRP.

period. Global tyrosine phosphorylation of proteins in platelets derived from CRP-stimulated $Cc2^{-/-}$ and wild-type mice was measured. Several tyrosine hyperphosphorylated proteins of 54, 56, 65, 71, 74, 83, and 93 kDa apparent molecular mass were detected in $Cc2^{-/-}$ in response to CRP stimulation for 15 seconds to 3 minutes by comparison with wild-type platelets (Figure 5A). Furthermore, PLCγ2, Src and Syk tyrosine phosphorylation was measured after CRP and Rhod-stimulation for 0 to 90 seconds by immunoprecipitation and western blot analysis with phosphotyrosine antibodies. As is shown in Figure 5B, CRP-stimulated $Cc2^{-/-}$ platelets showed a fivefold increase in PLCγ2 tyrosine phosphorylation (0.5230 ± 0.014 vs 0.1340 ± 0.004; ***$P < .001$; n = 3; Figure 5Ba), a threefold increase in Src tyrosine phosphorylation (0.4573 ± 0.051 vs 0.2710 ± 0.027; *$P < .05$; n = 3; Figure 5Bb), and a 3.5-fold increase in Syk tyrosine phosphorylation (0.5437 ± 0.011 vs 0.1167 ± 0.008; ***$P < .001$; n = 3; Figure 5Bc) compared with wild-type platelets. In addition, PLCγ2 and Syk tyrosine phosphorylation was measured after Rhod stimulation for 0 to 90 seconds. As is shown in Figure 5C, Rhod-stimulated $Cc2^{-/-}$ platelets showed a 3.5-fold increase in PLCγ2 tyrosine phosphorylation (0.4063 ± 0.014 vs 0.1093 ± 0.034; **$P < .01$; n = 3; Figure 5Ca) and a threefold increase in Syk tyrosine phosphorylation (0.4050 ± 0.060 vs 0.1508 ± 0.029; **$P < .01$; n = 3; Figure 5Cb) in the presence of equivalent PLCγ2, Src, and Syk, and ERK-2 antigens (bottom panel) compared with wild-type platelets. These data are consistent with CEACAM2 playing a role in attenuating platelet GPVI-collagen interactions and the CLEC-2 ITAM signaling pathway.

CEACAM2 regulation of platelet thrombus formation is dependent on platelet-collagen interactions under arterial flow in vitro

Because $Cc2^{-/-}$ platelets displayed strong adhesion on immobilized type I collagen, in vitro flow studies were performed to determine the functional role of CEACAM2 in modulating platelet thrombus formation. Rhodamine-labeled whole blood from both wild-type and $Cc2^{-/-}$ mice was perfused onto immobilized type I fibrillar collagen at an arterial shear rate of $1800 \, s^{-1}$. After 4 minutes of blood perfusion, thrombi images were recorded in real time for wild-type and $Cc2^{-/-}$ platelets (Figure 6A). Z-stacks were deconvolved and parameters of thrombus area, height, and volume were determined. $Cc2^{-/-}$ platelets exhibited a significant increase in thrombus area compared with wild-type platelets (2303 ± 470.6 vs $907.2 \pm 87.26 \, \mu m^2$; ***$P < .001$; n = 10; figure not shown). Similarly, $Cc2^{-/-}$ platelets showed increased kinetics in thrombus volume over time compared with wild-type platelets (30480 ± 3822 vs $12480 \pm 588.2 \, \mu m^3$; ***$P < .001$; n = 10; Figure 6B). Because $Cc2^{-/-}$ females are obese and insulin resistant[16] and $Cc2^{-/-}$ males are lean and insulin sensitive,[17] and platelet activation is associated with diabetes, we sex-stratified the in vitro thrombus formation to investigate a potential sexual dimorphic effect. $Cc2^{-/-}$ platelets showed increased thrombus volume in both male and female mice compared with wild-type platelets (*$P < .05$; Figure 6C). Collectively, platelet adhesion onto immobilized type I collagen under arterial flow demonstrated that CEACAM2 is important in regulating platelet thrombus formation in vitro under flow.

CEACAM2 acts as a negative regulator of platelet thrombus formation in vivo

The Ig-ITIM superfamily members, PECAM-1 and CEACAM1, negatively regulate platelet GPVI-collagen interactions and thrombus
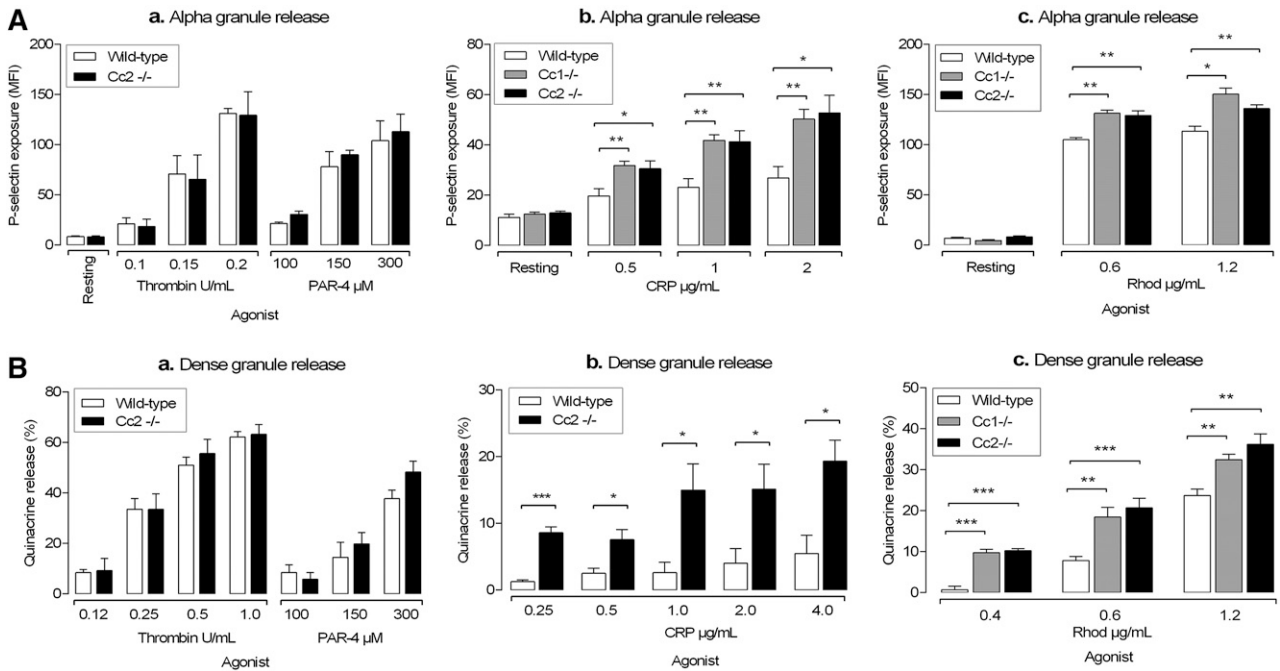
Figure 3. $Cc2^{-/-}$ platelets display enhanced α and dense granule release after stimulation with GPVI and CLEC-2–selective agonists, CRP and Rhod. (A) Surface expression of P-selectin as a marker of α granule release was determined for washed platelets stimulated by several agonists: (a) Thrombin (0.125-0.25 U/mL), PAR-4 agonist peptide (100-300 μM), (b) CRP (0.5-2.0 μg/mL), and (c) Rhod (0.6-1.2 μg/mL). Then they were stained with FITC-conjugated P-selectin mAb for wild-type, $Cc1^{-/-}$, and $Cc2^{-/-}$ platelets. FITC-labeled samples were analyzed on an FACS Canto II flow cytometer. Results are representative of 3 independent experiments (*$P < .05$, **$P < .01$; n = 4). (B) Platelet-dense granule exocytosis measured by release of fluorescent quinacrine by flow cytometry. Washed platelets (1×10^8/mL) were derived from both wild-type and $Cc2^{-/-}$ mice and were stimulated with either no agonist or agonist. (a) Thrombin (0.125-1.0 U/mL) or PAR-4 agonist peptide (100-300 μM) or (b) CRP (0.25-4.0 μg/mL). (c) Wild-type, $Cc1^{-/-}$, and $Cc2^{-/-}$ platelets were stimulated by Rhod (0.4-1.2 μg/mL). Samples were analyzed on an FACS Canto II flow cytometer. Data are reported as percentage quinacrine release and are representative of 4 independent experiments (*$P < .05$, **$P < .01$, ***$P < .001$; n = 4).

growth in vitro and in vivo.[2,13] Thus, we tested whether CEACAM2 plays a similar role in platelet thrombus formation in vivo. We used the $FeCl_3$ vascular injury model of mesenteric arterioles and laser-induced vascular injury of cremaster arterioles for wild-type vs $Cc2^{-/-}$ mice. We observed thrombus growth characteristics by measuring fluorescently labeled platelets bound at injury sites.
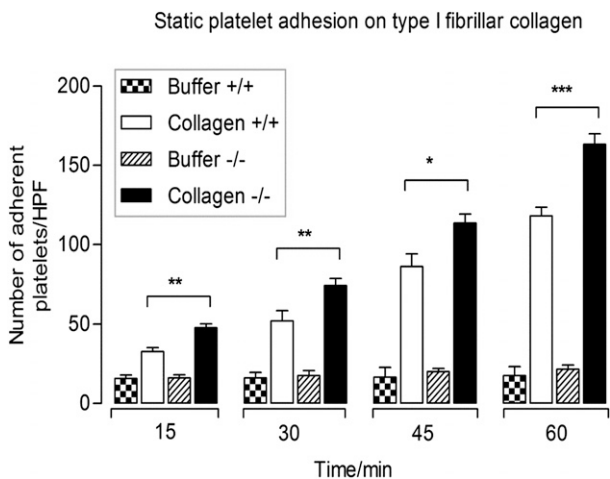

Figure 4. $Cc2^{-/-}$ platelets display enhanced static adhesion on immobilized type I collagen. Time course of wild-type and $Cc2^{-/-}$ platelet adhesion to either buffer control or type I collagen (50 μg/mL) in the absence of magnesium for 15, 30, 45, and 60 minutes at 37°C. Nonadherent platelets were removed and adherent platelets were measured as described in Materials and methods. The data represent 4 independent experiments. Note that $Cc2^{-/-}$ platelets show a higher level of platelet adhesion to type I fibrillar collagen than wild-type platelets ($^{+/+}$) at all time points (*$P < .05$, **$P < .01$, ***$P < .001$; n = 4).

$Cc2^{-/-}$ arterioles showed increased thrombus growth and stability over a 10-minute period, and they had a larger surface coverage of platelets (thrombus area) than wild-type arterioles (Figure 7Aa). Furthermore, thrombus volume in $Cc2^{-/-}$ arterioles was significantly larger (166900 ± 7601 vs 120500 ± 2390 μm^3; ***$P < .0001$; n = 30; Figure 7Ab-c), and the stability score of thrombi formed in $Cc2^{-/-}$ arterioles was higher than in wild-type arterioles (7.267 ± 0.143 vs 3.493 ± 0.136; ***$P < .0001$; n = 30; Figure 7Ad). $Cc2^{-/-}$ arterioles showed no difference in the time to first thrombus larger than 20 μm^2 and time to vessel occlusion ($P > .05$; n = 30; data not shown) when compared with wild-type arterioles. Typically, after laser-induced vascular injury of cremaster arterioles, $Cc2^{-/-}$ and $Cc1^{-/-}$ arterioles had greater thrombus volume compared with wild-type arterioles (37355 ± 702.6 vs 31956 ± 785.1 vs 15578 ± 543.7, respectively; ***$P < .0001$; n = 30; Figure 7Ba), and they were more stable (5.733 ± 0.143 vs 4.80 ± 0.010 vs 2.967 ± 0.0894, respectively; ***$P < .0001$; n = 30; Figure 7Bb).

Because GPVI collagen receptors interact directly with type I collagen during thrombus formation, GPVI was depleted in vivo for 5 days before $FeCl_3$ injury treatment with the GPVI neutralizing antibody, JAQ1 (100 μg/mouse).[29] GPVI depletion was confirmed using western blotting of wild-type and $Cc2^{-/-}$ platelet lysates (data not shown). Different cohorts of wild-type and $Cc2^{-/-}$ mice were treated with negative isotype control IgG (100 μg/mouse). Compared with wild-type, isotype-treated, or untreated wild-type arterioles, JAQ1-treated $Cc2^{-/-}$ arterioles displayed significant differences for a twofold reduction in thrombus volume and stability score (***$P < .001$; n = 10; Figure 7Ca). Importantly, upon JAQ1 treatment, $Cc2^{-/-}$ arterioles displayed reversal of the increased thrombus stability and growth phenotype compared with wild-type arterioles (***$P < .001$; n = 10; Figure 7Cb). In general, these

Figure 5. $Cc2^{-/-}$ platelets show hyperphosphorylated proteins after GPVI and CLEC-2–selective agonists, CRP and Rhod, stimulation over time. (A) Platelets (3×10^8/mL) from wild-type and $Cc2^{-/-}$ mice were stimulated with 10 μg/mL of CRP at 37 °C for 3 minutes. Platelet lysate of 30 μg was then loaded onto a 10% (wt/vol) SDS-PAGE gel. Then western blotting was performed to measure tyrosine phosphorylation using 1:5000 of HRP-conjugated anti-phosphotyrosine RC20 antibody. A protein-loading control (bottom panel) blot was stripped and reprobed using anti-Erk-1/2 Ab for detection of Erk-1 and -2 antigens. The data shown are a representative blot of similar results for 3 independent experiments. (B) Tyrosine phosphorylation of PLCγ2, Src, and Syk was detected from platelet lysate after stimulation with 10 μg/mL of CRP vs resting at time 0 and 90 seconds. Immunoprecipitation of PLCγ2, Src, and Syk from platelet lysates was performed followed by immunoblotting to detect (a) p-PLCγ2, using 1:5000 of an HRP-conjugated anti-phosphotyrosine RC20 antibody, (b) p-Src, using 1:2000 of antiphospho Src and 1:20 000 of anti-rabbit, and (c) p-Syk, using 1:20 000 of an HRP-conjugated anti-phosphotyrosine 4G10 antibody. PLCγ2, Src, and Syk antigens (bottom panel; a-c) loading control were confirmed by reprobing with polyclonal anti-PLCγ2, anti-Src, and anti-Syk antibodies, respectively. The relative intensity of tyrosine-phosphorylated PLCγ2, Src, and Syk was quantified by ImageJ software, version 1.46r. The data shown are a representative blot of similar results for 3 independent experiments. (C) Tyrosine phosphorylation of PLCγ2 and Syk was detected from platelet lysate after stimulation with 1.2 μg/mL of Rhod vs resting at time 0 and 90 seconds as described in (B).
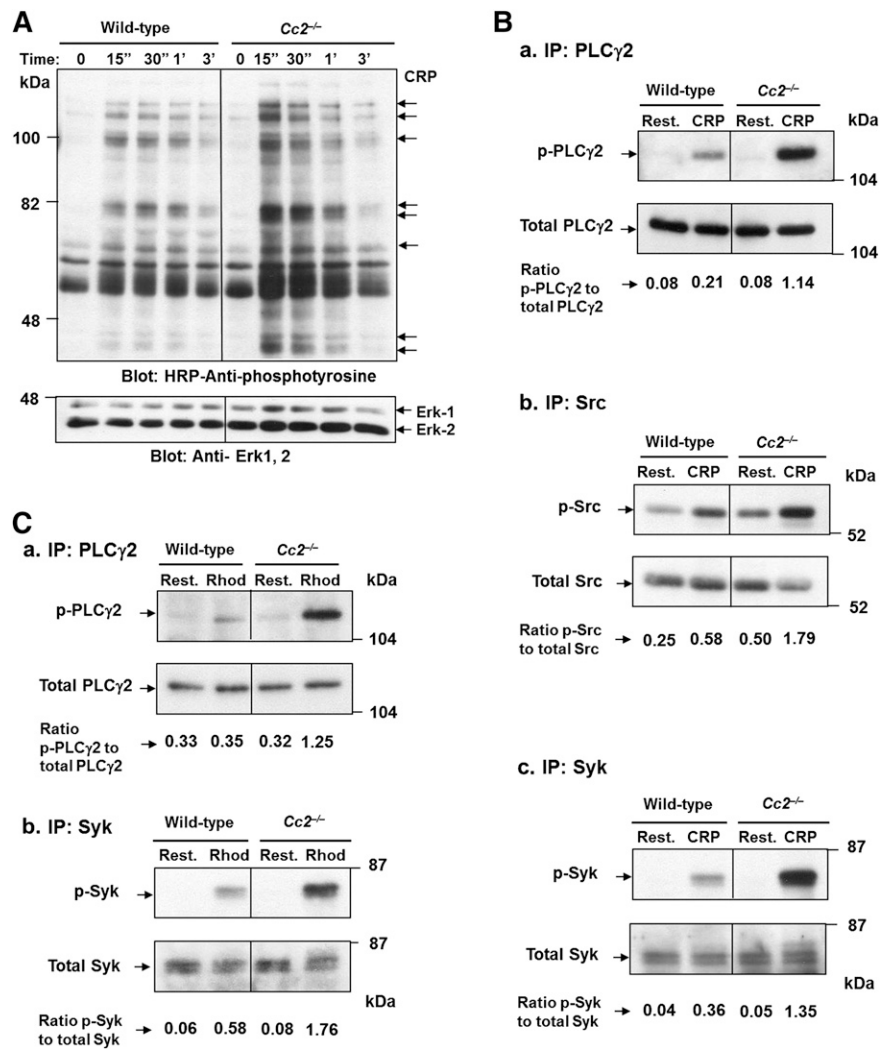
results suggest that CEACAM2, in tandem with GPVI, contributes to the more stable thrombus phenotype.

Discussion

Maintaining platelet quiescence requires a balance between activation and inhibition-signaling events mediated by ITAM and regulated by ITIM-bearing receptor signaling. Healthy arterial endothelium is able to provide powerful inhibitory signaling to platelets via release of bioactive nitrous oxide (NO) and prostaglandin I₂ (PGI₂). However, upon endothelial damage or disease, where bioactive NO and PGI₂ concentrations are low, collectively platelet ITIM-bearing receptors play an important role as negative regulators.[1] In addition, like in the immune system, a homeostatic balance is required between activation and inhibition and this is provided in platelets through ITAM- and ITIM-bearing receptor pathways.[1] This stimulates the activation mechanisms to produce pathological thrombus formation. Under these circumstances, platelets may provide the inhibitory signaling mediated via cell-contact events. Platelets contain at least 4 ITIM-bearing receptors: PECAM-1, CEACAM1, G6B, and TREM-like transcript 1.[2,3,13-15,39] Although individually these exert moderate inhibition of collagen and thrombin signaling in platelets, collectively they regulate the cell-contact signaling events involved in the initiation of platelet thrombus formation to limit occlusive pathological thrombi.

To our knowledge, this study provides the first report of a new ITIM-bearing receptor, CEACAM2 in murine platelets. The key findings in this study are that CEACAM2 is expressed as the CC2-2L form in platelets (Figure 1C), similar to other cell types such as ventromedial hypothalamus[16] and spermatids.[18] Moreover, CEACAM2 is expressed on the surface as well as in the intracellular pool of resting platelets (Figure 1A). In vitro data show that CEACAM2 can negatively regulate the collagen GPVI and CLEC-2 ITAM–signaling pathway in platelets. Under in vitro conditions of physiological arterial shear flow, absence of CEACAM2 results in increased surface coverage of platelets on immobilized type I collagen (Figure 6A). There was no evidence of sexual dimorphism with regard to this enhanced thrombus growth phenotype of $Cc2^{-/-}$ platelets. In addition, using several models of microvascular thrombosis in vivo, we show that Ceacam2 deletion results in larger and more stable thrombi than in wild-type mice, and that this at least partly depends on the presence of GPVI (Figure 7). Collectively, these findings of the initial characterization of CEACAM2 in murine platelets and its ability to negatively regulate platelet-collagen interactions in vitro and in vivo are reminiscent of the functions of the other related ITIM-bearing receptor, CEACAM1. These 2 receptors share similarities in structure and function in many biological systems, particularly in
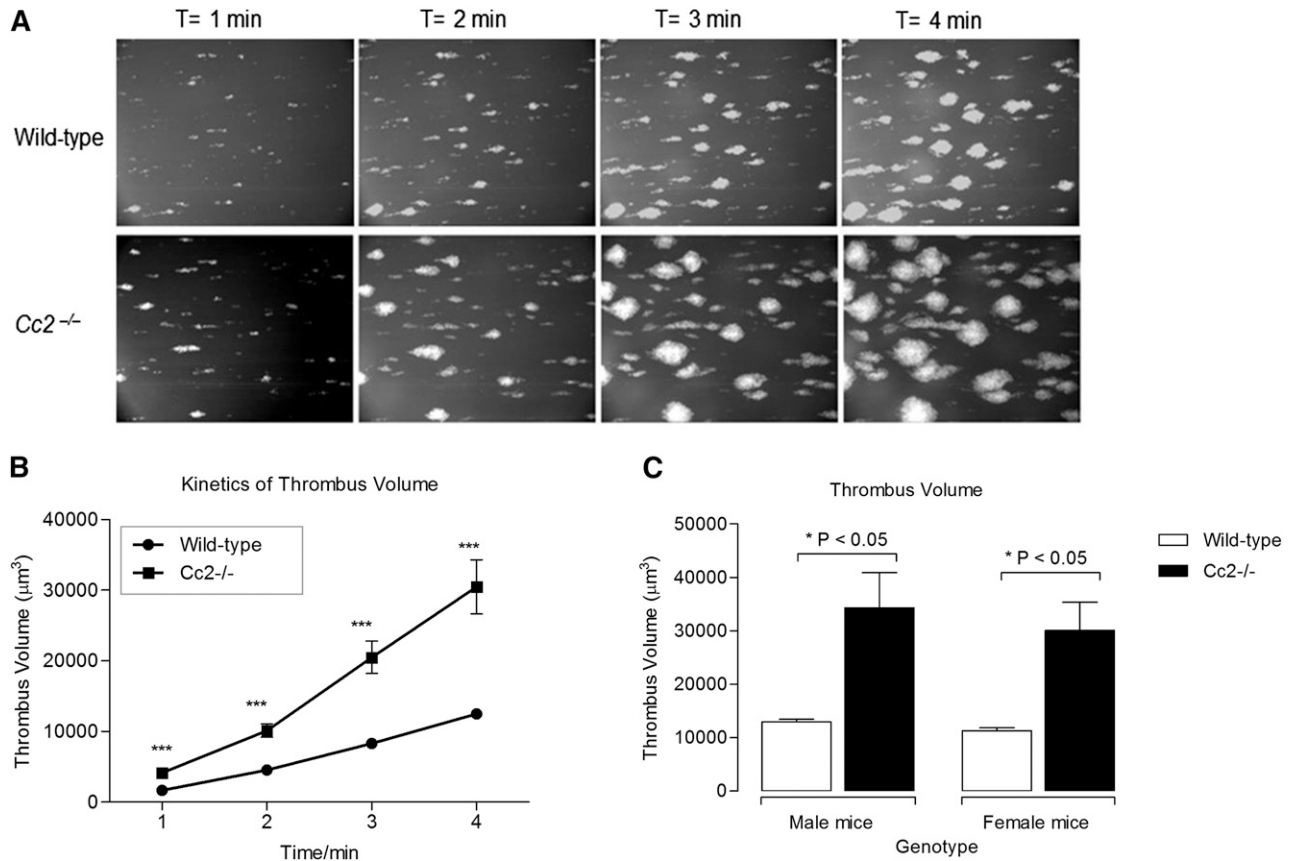
Figure 6. $Cc2^{-/-}$ platelets display greater adhesion and thrombus formation under arterial flow on immobilized type I collagen. (A-C) Rhodamine-labeled whole blood of wild-type and $Cc2^{-/-}$ mice was perfused over 500 µg/mL type I fibrillar collagen–coated µ-slide III$^{0.1}$ at a shear wall flow rate of 1800 s^{-1}. Z-stack images were recorded over 4 minutes with a Zeiss Axiovert microscope captured with Axiocam MRm camera and analyzed using Zeiss Axiovision Rel4.6 software. Thrombi formed were analyzed by deconvolution and 3-D reconstructions. (A) Images of in vitro thrombus formation under arterial flow on immobilized type I fibrillar collagen for both wild-type and $Cc2^{-/-}$ platelets over 4 minutes. (B) Kinetics of thrombus volume (µm^3) over time was derived by multiplying thrombus area (µm^2) with thrombus height (µm) for both wild-type and $Cc2^{-/-}$ platelets (30 480 ± 3822 vs 12 480 ± 588.2 µm^3; ***$P < .001$; at 4 minutes; n = 10). (C) Thrombus volume (µm^3) data from (B) was stratified according to sex, both male and female, for both wild-type and $Cc2^{-/-}$ platelets at the 4-minutes time point (*$P < .05$; n = 5 per group).

their ability to act as inhibitory co-receptors to modulate ITAM-associated signaling pathways. Essentially, $Cc1^{-/-}$ and $Cc2^{-/-}$ have similar phenotypes in platelet GPVI–collagen interactions and CLEC-2 interactions. Moreover, *Ceacam2* deletion was associated with CRP- and Rhod-stimulated platelets producing tyrosine hyper-tyrosine phosphorylation of PLC-γ2, Src, and Syk; all components upstream and downstream of either GPVI or CLEC-2 ITAM–associated signaling pathways (Figure 5B-C). This is consistent with CEACAM2 acting as an ITIM-bearing receptor in platelets to down-modulate ITAM-associated signaling, similarly to CEACAM1, the ITIM-containing tail of which is almost identical to that of CEACAM2.

Whether CEACAM2 regulates thrombin signaling in platelets remains unclear. In response to thrombin (at 0.25-1.0 U/mL), $Cc2^{-/-}$ platelets had comparable amplitude and slope of thrombin-mediated aggregation response compared with wild-type platelets (Figure 2B). In addition, G protein–coupled receptor platelet aggregation mediated by ADP, thrombin, and PAR-4 agonist peptide were comparable in $Cc2^{-/-}$ and wild-type platelets (Figure 2). Although these results would argue against CEACAM2 regulating thrombin signaling, more studies using thrombin at subthreshold concentrations are needed to fully address this question. Moreover, the laser injury model used in this study is mediated by the thrombin:tissue factor inflammatory process, and the $Cc2^{-/-}$ arterioles had increased thrombi that were more stable under these conditions (Figure 7B). Thus, more studies

are needed to investigate whether CEACAM2 affects the thrombin-signaling pathway.

Unlike human platelets, murine platelets lack the low-affinity IgG receptor, FcgammaRIIa, but contain 2 ITAM-bearing receptors, GPVI/FcR γ chain and CLEC-2. CEACAM2 also negatively regulates signaling of CLEC-2, which has been shown to play a role in thrombus stabilization.[40] Based on our in vivo mouse thrombus models, we show that $Cc2^{-/-}$ arterioles have larger thrombi that are more stable in response to type I collagen exposure (ie, ferric chloride–induced vascular injury of mesenteric arterioles; Figure 7A) and thrombin-driven processes without type I collagen exposure (ie, laser-induced injury of cremaster muscle arterioles[41,42]; Figure 7B). This was also the case for $Cc1^{-/-}$ (in this study) and PECAM-1$^{-/-}$ arterioles.[43] Although GPVI depletion resulted in the reversal of thrombus growth, thrombus stability was less affected, indicating the involvement of other potential mechanisms regulating thrombus stability (Figure 7C).

In conclusion, this study demonstrates the presence of a new ITIM-bearing receptor, CEACAM2 (predominantly CC2-2L), in murine platelets that negatively regulates collagen GPVI and CLEC-2 signaling in addition to thrombus growth and stability in vitro and in vivo. Like CEACAM1, CEACAM2 limits thrombi formation under conditions of type I collagen exposure, such as atherosclerotic plaque rupture. Further studies are required to decipher other mechanisms of its role in platelet function, thrombus stabilization, and wound healing.
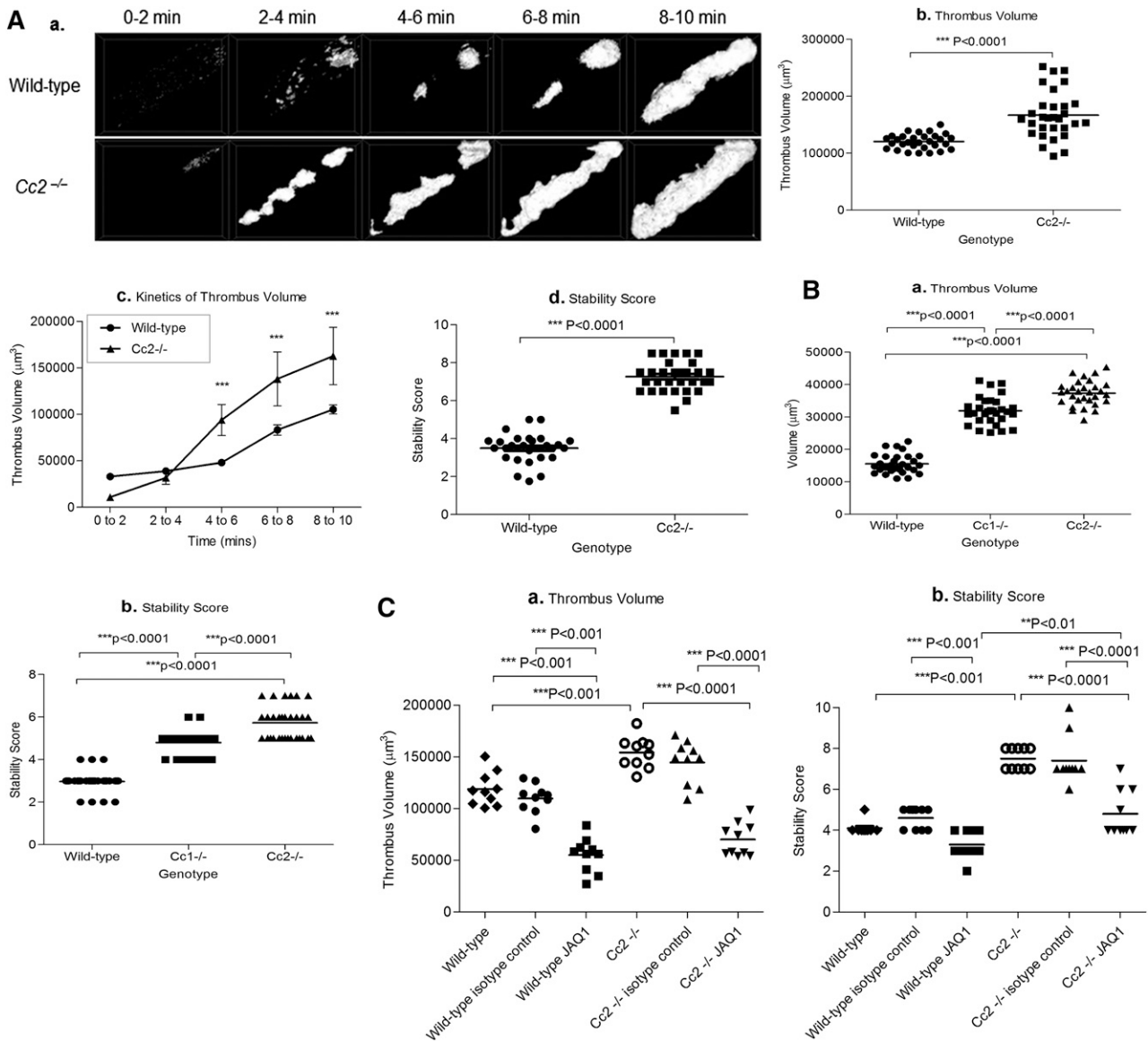
Figure 7. $Cc2^{-/-}$ mice display larger and more stable thrombi in vivo. (Aa) Z-stack thrombus formation images of $FeCl_3$-induced vascular injury was monitored in arterioles of wild-type vs $Cc2^{-/-}$ mice over 10 minutes. The different lengths of time after $FeCl_3$ application are specified. Note that thrombi are larger in $Cc2^{-/-}$ arterioles over time compared with wild-type control arterioles (n = 30). (b) Quantitative analysis of arterial thrombogenesis of wild-type (●) vs $Cc2^{-/-}$ (■) arterioles. $Cc2^{-/-}$ arterioles displayed a significantly larger thrombus volume at 10 minutes compared with wild-type arterioles (166 900 ± 7601 vs 120500 ± 2390 μm^3; ***P < .0001; n = 30). (c) The kinetics of thrombus volume of wild-type vs $Cc2^{-/-}$ arterioles over time was reliably measured. $Cc2^{-/-}$ arterioles were significantly increased at 4 to 10 minutes compared with wild-type arterioles. (d) The thrombus stability was scored from 1 to 10, with 1 being 0% to 10% occupancy and 10 being 91% to 100% occupancy (ie, complete vessel occlusion) visualized over time. $Cc2^{-/-}$ arterioles showed greater stability in thrombi formed (7.267 ± 0.143 vs 3.493 ± 0.136; ***P < .0001; n = 30). (Ba-b) Platelet thrombus formation in response to laser-induced injury in wild-type, $Cc1^{-/-}$, and $Cc2^{-/-}$ arterioles. Thrombus volume in $Cc2^{-/-}$ and $Cc1^{-/-}$ arterioles was significantly greater than wild-type arterioles (37 355 ± 702.6 vs 31 956 ± 785.1 vs 15 578 ± 543.7, respectively; ***P < .0001; n = 30) and displayed greater stability in thrombi formed (5.733 ± 0.143 vs 4.80 ± 0.010 vs 2.967 ± 0.0894, respectively; ***P < .0001; n = 30). (Ca-b) Thrombus formation in response to $FeCl_3$ after inhibition of mouse GPVI with specific monoclonal antibody (mAb) JAQ1 administration to wild-type and $Cc2^{-/-}$ mice compared with control IgG-treated wild-type and $Cc2^{-/-}$ or untreated wild-type and $Cc2^{-/-}$ mice. Compared with untreated $Cc2^{-/-}$ or control IgG-treated $Cc2^{-/-}$ arterioles, JAQ1-treated $Cc2^{-/-}$ arterioles displayed around a twofold smaller thrombus volume at 10 minutes (154 300 ± 4741 vs 144 600 ± 6613 vs 70 050 ± 5077 μm^3, respectively; ***P < .0001; n = 10 arterioles from 3 mice per group) and around a twofold lower stability score at 10 minutes (7.500 ± 0.166 vs 7.400 ± 0.371 vs 4.800 ± 0.359, respectively; ***P < .0001; n = 10 arterioles from 3 mice per group). In contrast, compared with untreated wild-type or control IgG-treated wild-type arterioles, JAQ1-treated wild-type arterioles displayed around a threefold smaller thrombus volume at 10 minutes (118 700 ± 5102 vs 109 800 ± 4497 vs 55 080 ± 5269 μm^3, respectively; ***P < .0001; n = 10 arterioles from 3 mice per group) and a moderately lower stability score at 10 minutes (4.100 ± 0.100 vs 4.600 ± 0.163 vs 3.300 ± 0.213, respectively; **P < .01; n = 10 arterioles from 3 mice per group).

Acknowledgments

Authorship

References

1. Jones CI, Barrett NE, Moraes LA, Gibbins JM, Jackson DE. Endogenous inhibitory mechanisms and the regulation of platelet function. *Methods Mol Biol.* 2012;788:341-366.

2. Jones KL, Hughan SC, Dopheide SM, Farndale RW, Jackson SP, Jackson DE. Platelet endothelial cell adhesion molecule-1 is a negative regulator of platelet-collagen interactions. *Blood.* 2001;98(5):1456-1463.

3. Patil S, Newman DK, Newman PJ. Platelet endothelial cell adhesion molecule-1 serves as an inhibitory receptor that modulates platelet responses to collagen. *Blood.* 2001;97(6):1727-1732.

4. Cicmil M, Thomas JM, Leduc M, Bon C, Gibbins JM. Platelet endothelial cell adhesion molecule-1 signaling inhibits the activation of human platelets. *Blood.* 2002;99(1):137-144.

5. Dhanjal TS, Ross EA, Auger JM, et al. Minimal regulation of platelet activity by PECAM-1. *Platelets.* 2007;18(1):56-67.

6. Pao LI, Badour K, Siminovitch KA, Neel BG. Nonreceptor protein-tyrosine phosphatases in immune cell signaling. *Annu Rev Immunol.* 2007;25:473-523.

7. Chemnitz JM, Parry RV, Nichols KE, June CH, Riley JL. SHP-1 and SHP-2 associate with immunoreceptor tyrosine-based switch motif of programmed death 1 upon primary human T cell stimulation, but only receptor ligation prevents T cell activation. *J Immunol.* 2004;173(2):945-954.

8. Okazaki T, Maeda A, Nishimura H, Kurosaki T, Honjo T. PD-1 immunoreceptor inhibits B cell receptor-mediated signaling by recruiting src homology 2-domain-containing tyrosine phosphatase 2 to phosphotyrosine. *Proc Natl Acad Sci USA.* 2001;98(24):13866-13871.

9. Hamerman JA, Lanier LL. Inhibition of immune responses by ITAM-bearing receptors. *Sci STKE.* 2006;2006(320):re1.

10. Abram CL, Lowell CA. The expanding role for ITAM-based signaling pathways in immune cells. *Sci STKE.* 2007;2007(377):re2.

11. Suzuki-Inoue K, Fuller GL, García A, et al. A novel Syk-dependent mechanism of platelet activation by the C-type lectin receptor CLEC-2. *Blood.* 2006;107(2):542-549.

12. Séverin S, Pollitt AY, Navarro-Nuñez L, et al. Syk-dependent phosphorylation of CLEC-2: a novel mechanism of hem-immunoreceptor tyrosine-based activation motif signaling. *J Biol Chem.* 2011;286(6):4107-4116.

13. Wong C, Liu Y, Yip J, et al. CEACAM1 negatively regulates platelet-collagen interactions and thrombus growth in vitro and in vivo. *Blood.* 2009;113(8):1818-1828.

14. Newland SA, Macaulay IC, Floto AR, et al. The novel inhibitory receptor G6B is expressed on the surface of platelets and attenuates platelet function in vitro. *Blood.* 2007;109(11):4806-4809.

15. Washington AV, Schubert RL, Quigley L, et al. A TREM family member, TLT-1, is found exclusively in the alpha-granules of megakaryocytes and platelets. *Blood.* 2004;104(4):1042-1047.

16. Heinrich G, Ghosh S, Deangelis AM, et al. Carcinoembryonic antigen-related cell adhesion molecule 2 controls energy balance and peripheral insulin action in mice. *Gastroenterology.* 2010;139(2):644-652, e1.

17. Patel PR, Ramakrishnan SK, Kaw MK, et al. Increased metabolic rate and insulin sensitivity in male mice lacking the carcino-embryonic antigen-related cell adhesion molecule 2. *Diabetologia.* 2012;55(3):763-772.

18. Salaheldeen E, Kurio H, Howida A, Iida H. Molecular cloning and localization of a CEACAM2 isoform, CEACAM2-L, expressed in spermatids in mouse testis. *Mol Reprod Dev.* 2012;79(12):843-852.

19. Han E, Phan D, Lo P, et al. Differences in tissue-specific and embryonic expression of mouse Ceacam1 and Ceacam2 genes. *Biochem J.* 2001;355(Pt 2):417-423.

20. Robitaille J, Izzi L, Daniels E, Zelus B, Holmes KV, Beauchemin N. Comparison of expression patterns and cell adhesion properties of the mouse biliary glycoproteins Bbgp1 and Bbgp2. *Eur J Biochem.* 1999;264(2):534-544.

21. Beauchemin N, Kunath T, Robitaille J, et al. Association of biliary glycoprotein with protein tyrosine phosphatase SHP-1 in malignant colon epithelial cells. *Oncogene.* 1997;14(7):783-790.

22. Huber M, Izzi L, Grondin P, et al. The carboxyl-terminal region of biliary glycoprotein controls its tyrosine phosphorylation and association with protein-tyrosine phosphatases SHP-1 and SHP-2 in epithelial cells. *J Biol Chem.* 1999;274(1):335-344.

23. Pasquet JM, Quek L, Pasquet S, et al. Evidence of a role for SHP-1 in platelet activation by the collagen receptor glycoprotein VI. *J Biol Chem.* 2000;275(37):28526-28531.

24. Leung N, Turbide C, Olson M, Marcus V, Jothy S, Beauchemin N. Deletion of the carcinoembryonic antigen-related cell adhesion molecule 1 (Ceacam1) gene contributes to colon tumor progression in a murine model of carcinogenesis. *Oncogene.* 2006;25(40):5527-5536.

25. Yan HC, Pilewski JM, Zhang Q, DeLisser HM, Romer L, Albelda SM. Localization of multiple functional domains on human PECAM-1 (CD31) by monoclonal antibody epitope mapping. *Cell Adhes Commun.* 1995;3(1):45-66.

26. Nieswandt B, Bergmeier W, Schulte V, Rackebrandt K, Gessner JE, Zirngibl H. Expression and function of the mouse collagen receptor glycoprotein VI is strictly dependent on its association with the FcRgamma chain. *J Biol Chem.* 2000;275(31):23998-24002.

27. Mendrick DL, Kelly DM, duMont SS, Sandstrom DJ. Glomerular epithelial and mesangial cells differentially modulate the binding specificities of VLA-1 and VLA-2. *Lab Invest.* 1995;72(3):367-375.

28. Bergmeier W, Rackebrandt K, Schröder W, Zirngibl H, Nieswandt B. Structural and functional characterization of the mouse von Willebrand factor receptor GPIb-IX with novel monoclonal antibodies. *Blood.* 2000;95(3):886-893.

29. Massberg S, Gawaz M, Grüner S, et al. A crucial role of glycoprotein VI for platelet recruitment to the injured arterial wall in vivo. *J Exp Med.* 2003;197(1):41-49.

30. Yasuda M, Hasunuma Y, Adachi H, et al. Expression and function of fibronectin binding integrins on rat mast cells. *Int Immunol.* 1995;7(2):251-258.

31. Trowbridge IS, Lesley J, Schulte R, Hyman R, Trotter J. Biochemical characterization and cellular distribution of a polymorphic, murine cell-surface glycoprotein expressed on lymphoid tissues. *Immunogenetics.* 1982;15(3):299-312.

32. Maecker HT, Todd SC, Levy S. The tetraspanin superfamily: molecular facilitators. *FASEB J.* 1997;11(6):428-442.

33. Wee JL, Jackson DE. The Ig-ITIM superfamily member PECAM-1 regulates the "outside-in" signaling properties of integrin α(IIb)β3 in platelets. *Blood.* 2005;106(12):3816-3823.

34. Yuan Y, Kulkarni S, Ulsemer P, et al. The von Willebrand factor-glycoprotein Ib/V/IX interaction induces actin polymerization and cytoskeletal reorganization in rolling platelets and glycoprotein Ib/V/IX-transfected cells. *J Biol Chem.* 1999;274(51):36241-36251.

35. Jackson DE, Ward CM, Wang R, Newman PJ. The protein-tyrosine phosphatase SHP-2 binds platelet/endothelial cell adhesion molecule-1 (PECAM-1) and forms a distinct signaling complex during platelet aggregation. Evidence for a mechanistic link between PECAM-1- and integrin-mediated cellular signaling. *J Biol Chem.* 1997;272(11):6986-6993.

36. Goschnick MW, Lau LM, Wee JL, et al. Impaired "outside-in" integrin alphaIIbbeta3 signaling and thrombus stability in TSSC6-deficient mice. *Blood.* 2006;108(6):1911-1918.

37. Dubois C, Panicot-Dubois L, Gainor JF, Furie BC, Furie B. Thrombin-initiated platelet activation in vivo is vWF independent during thrombus formation in a laser injury model. *J Clin Invest.* 2007;117(4):953-960.

38. Orlowski E, Chand R, Yip J, et al. A platelet tetraspanin superfamily member, CD151, is required for regulation of thrombus growth and stability in vivo. *J Thromb Haemost.* 2009;7(12):2074-2084.

39. Nédellec P, Dveksler GS, Daniels E, et al. Bgp2, a new member of the carcinoembryonic antigen-

related gene family, encodes an alternative receptor for mouse hepatitis viruses. *J Virol.* 1994; 68(7):4525-4537.

40. Suzuki-Inoue K, Inoue O, Ozaki Y. Novel platelet activation receptor CLEC-2: from discovery to prospects. *J Thromb Haemost.* 2011;9(Suppl 1):44-55.

41. Atkinson BT, Jasuja R, Chen VM, Nandivada P, Furie B, Furie BC. Laser-induced endothelial cell activation supports fibrin formation. *Blood.* 2010; 116(22):4675-4683.

42. Dubois C, Panicot-Dubois L, Merrill-Skoloff G, Furie B, Furie BC. Glycoprotein VI-dependent

and -independent pathways of thrombus formation in vivo. *Blood.* 2006;107(10): 3902-3906.

43. Falati S, Patil S, Gross PL, et al. Platelet PECAM-1 inhibits thrombus formation in vivo. *Blood.* 2006; 107(2):535-541.